Accepted Manuscript

Combining DNA-stabilized silver nanocluster synthesis with exonuclease III amplification allows label-free detection of coralyne

Cheng-Yu Lee, Shun-Wen Lin, Yi-Hsuan Wu, You-Zung Hsieh

PII: S0003-2670(18)30996-6

DOI: 10.1016/j.aca.2018.08.030

Reference: ACA 236204

To appear in: *Analytica Chimica Acta*

Received Date: 28 December 2017

Revised Date: 2 July 2018

Accepted Date: 14 August 2018

Please cite this article as: C.-Y. Lee, S.-W. Lin, Y.-H. Wu, Y.-Z. Hsieh, Combining DNA-stabilized silver nanocluster synthesis with exonuclease III amplification allows label-free detection of coralyne, *Analytica Chimica Acta* (2018), doi: 10.1016/j.aca.2018.08.030.

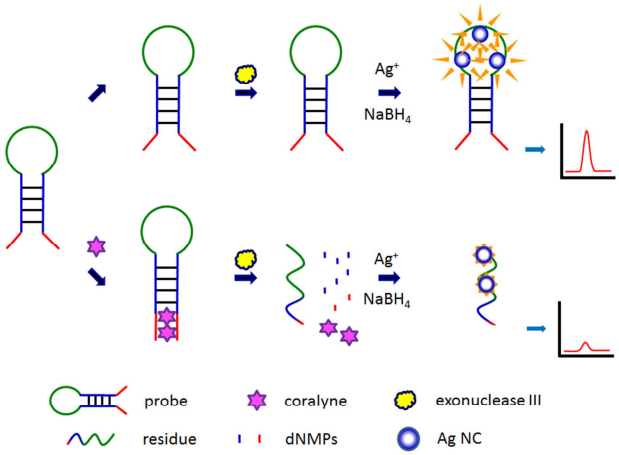

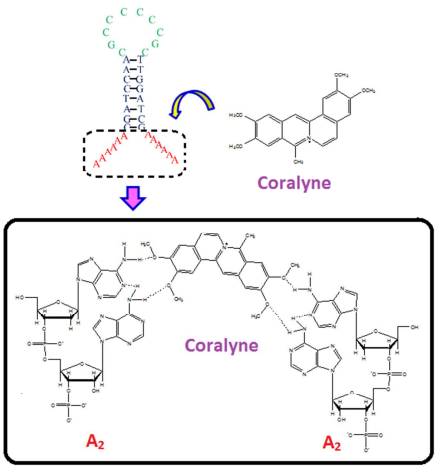

Combining DNA-stabilized silver nanocluster synthesis with exonuclease III amplification allows label-free detection of coralyne

Cheng-Yu Lee[1], Shun-Wen Lin[1], Yi-Hsuan Wu[1], You-Zung Hsieh*[,1,2]

[1]*Department of Applied Chemistry*

[2]*Center for Emergent Functional Matter Science*

National Chiao Tung University

Hsinchu, Taiwan, R.O.C.

Tel.: 886-3-5731785

Fax: 886-3-5723764

E-mail: yzhsieh@mail.nctu.edu.tw

Abstract

In this paper we describe a label-free biosensor for coralyne, prepared by combining DNA-stabilized silver nanoclusters (Ag NCs) with an exonuclease III amplification strategy. An artificial DNA probe having a polyadenine (poly-A) sequence at both the 3´- and 5´-ends was used as a probe to detect coralyne. In the absence of coralyne, the probe existed in a hairpin conformation that left both its 3´- and 5´-ends free. In the presence of coralyne, two adjacent adenine (A) bases in the poly-A sequence of the probe formed an A_2 unit and then coordinated with coralyne through non-Watson–Crick base pairing. The DNA probe, having captured coralyne, was subsequently digested by exonuclease III, even though the distance between the A_2 units in the A_2–coralyne–A_2 complex would be much larger than that found in common Watson–Crick base pairing. After digestion, the DNA probe became a single-stranded DNA (ssDNA) residue and released its captured coralyne. The liberated coralyne was then coordinated by another DNA probe having the hairpin conformation; as a result, many ssDNA residues formed after digestion. Two kinds of Ag NCs having different optical utilities were obtained: one corresponding to the hairpin conformational DNA probe and the other to the ssDNA residue. The difference in fluorescence intensity at 588 nm of these two kinds of Ag NCs reflected the concentration of coralyne. The linear range (on a logarithmic scale) for detecting coralyne spanned from 5 to 1000 nM, with an estimated detection limit of 1.83 nM.

Keywords: *coralyne biosensor; silver nanoclusters; DNA probe; exonuclease III amplification*

1. Introduction

In recent years, non-Watson–Crick base pairing has been used to design many oligonucleotide probes or molecular beacons for new types of biosensors. For example, a DNA sequence containing thymine (T)-rich units at both the 3´- and 5´-ends has been employed as a specific identification and detection probe for Hg^{2+} ions [1-3]; the formation of coordinated T–Hg^{2+}–T units (or not) led to the hairpin (or folded) form of the oligonucleotide probe, turning the sensor on (or off). A similar interaction between cytosine (C) and Ag^{+} ions has been used to synthesize DNA-stabilized silver nanoparticles or clusters through specific C–Ag^{+} recognition and coordination [4-7]. These kinds of DNA-stabilized silver nanocomposites have been used as, for example, critical materials for fluorescent [7-9] and electrochemical [5, 10] biosensors.

Alkaloids are abundant natural products; most of them display biological activity—for example, anti-oxidant, anti-bacterial, or anti-tumor properties. Isolated or synthesized alkaloids have been studied widely in several fields for many different purposes. Coralyne (5,6,7,8,13,13a-hexadehydro-8-methyl-2,3,10,11-tetramethoxyberbinium chloride) is a planar, protoberberine alkaloid. Protoberberines have the potential to be among the most useful alkaloids, exhibiting anti-tumor activities that have already led to the development of an anti-cancer drug [11-13]. Several similar compounds, including palmatine, berberine, and sanguinarine, are also notable for their high activities in pharmaceutical treatments. Among these compounds, coralyne has displayed superior efficacy in anti-tumor experiments as well as a low toxicity profile; as a result, it has attracted the attention of clinical researchers. The major role played by coralyne is related to the poisoning of topoisomerases I and II [14, 15]. Although in recent years there have been several approaches developed for detecting coralyne using various methods (Table S1), most of these analyses are complicated, in terms of their operating

processes, and time-consuming. Coralyne promotes non-traditional pairing of oligonucleotides having adenosine (A)-rich sequences [12, 16-18]. Two adjacent A units first interact to form an A_2 unit. In the presence of coralyne, two A_2 units recognize and bind a single coralyne molecule, forming an A_2–coralyne–A_2 complex [12, 16, 17], with a binding constant of 1.05×10^5 M^{-1} [14, 19, 20] that is much higher than that of a natural A–T base pair. Taking advantage of this non-Watson–Crick base pair interaction, the last decade has witnessed the development of several molecular beacons and methods for the detection of coralyne [15, 21-24].

Changing the size or shape of a nanomaterial leads to the changes in its physical and chemical properties. Fluorescence measurements can be applied for some noble metals, particularly gold or silver, when their nanocluster (NC) sizes are on the order of ten atoms, providing labels that function as alternatives to fluorescent dyes, quantum dots, and fluorescent proteins. These kinds of noble metal NCs have attracted great interest because of their high molar absorptions, good quantum yields, low cytotoxicity, and small dimensions. Nevertheless, there remain several drawbacks that limit the application of these NCs—in particular, low stability and low environmental tolerance. Petty et al. reported that DNA-stabilized silver nanoclusters (Ag NCs) can exhibit good stability without losing their fluorescence properties [25]. Furthermore, Ag NCs bind to DNA bases, rather than to the sugar-phosphate backbone [26, 27]. Among the four nucleoside bases, the affinity of DNA sequences to Ag NCs is strongest through their C residues. Taking advantage of such affinity has allowed tuning of the optical properties of DNA-stabilized Ag NCs through changes in the sequence of the DNA template [28]. Furthermore, the structure of the DNA template can determine the structure and size of the formed Ag NCs [29-31]. In addition, the fluorescence spectrum and intensity depend not only on the sequence of the DNA template but also on its structure. Several applications have been developed to exploit changes in the fluorescence properties of

DNA-stabilized Ag NCs [30-33]. These approaches provide a facile means of fabricating Ag NCs that display various fluorescence emission behaviors, while also implying that it should be possible to design novel biosensors based on these kinds of DNA-stabilized Ag NCs.

Fluorescent Ag NCs have been used as alternatives to fluorescent dyes in sensing and imaging systems because they are easy to prepare and because they possess size-dependent optical properties. In general, the photophysical properties of Ag NCs depend on their morphology, oxidation state, and surface ligands [32, 34, 35]. In addition, changes in their morphologies and sizes usually lead to variations in fluorescence intensity. Aggregation of Ag NCs can result in distinct fluorescence quenching phenomena and significantly decreased fluorescence intensities. Nevertheless, oligonucleotide loops can be used as protective materials that prevent Ag NCs from aggregating. Cytosine-rich oligonucleotide loops are preferred for the synthesis of fluorescent Ag NCs [36-38].

In this study, we designed a DNA probe as the critical recognition material of a label-free coralyne biosensor. This DNA probe binds to coralyne through the formation of an A_2–coralyne–A_2 complex. The distances between the A units in the A_2–coralyne–A_2 complexes were much longer than those found in regular base pairing. After exonuclease III had digested the coralyne-bound DNA probe, the DNA probe became a single-stranded DNA (ssDNA); this transformation affected the formation of Ag NCs. The reaction conditions for the synthesis of Ag NCs were chosen to maximize the difference in fluorescence. In particular, the change in the fluorescence intensity of the Ag NCs, measured at a value of λ_{max} of 588 nm, was related to the concentration of coralyne. The selectivity of this DNA probe for coralyne has also been investigated.

Scheme 1 displays the analytical protocol developed in this study. The designed DNA probe featured three sections. The first, containing six A units on each end of the

probe, is the poly-A section. This section, which served as the probing unit, was positioned at both termini of the DNA probe. In the presence of coralyne, one A_2 unit at each end of the designed DNA probe would bind with coralyne to form the double-stranded DNA (dsDNA) structure A_2–coralyne–A_2, leading to a blunt end of the DNA probe that was recognized and hydrolyzed by exonuclease III. The second section, next to the poly-A section, was a complementary sequence that formed the initial hairpin structure of the DNA probe, thereby positioning the two terminal poly-A sequences close together to ensure stronger binding of coralyne. The last section, the poly-C section [consisting of eight C bases and two guanine (G) bases], was present to function as a template to form Ag NCs with intense fluorescence; it remained in a crowded loop region prior to exonuclease III–mediated hydrolysis, indirectly providing a DNA probe capable of discriminating samples with or without coralyne. After binding coralyne, the DNA probe became susceptible to digestion by exonuclease III from its blunt 3´-termini, resulting in release of the target coralyne. The resulting conformational change—from hairpin/loop to ssDNA—provided DNA that stabilized the synthesis of Ag NCs, resulting in different fluorescence emission spectra being obtained in the presence and absence of coralyne. The change in fluorescence intensity corresponded to the concentration of coralyne. Thus, the system functioned as a label-free biosensor for coralyne. Moreover, the sensitivity of the developed assay was increased further by incorporating exonuclease III–promoted amplification cycling loops. Using both strategies, coralyne could be analyzed and quantified readily with high sensitivity.

1 **Y**

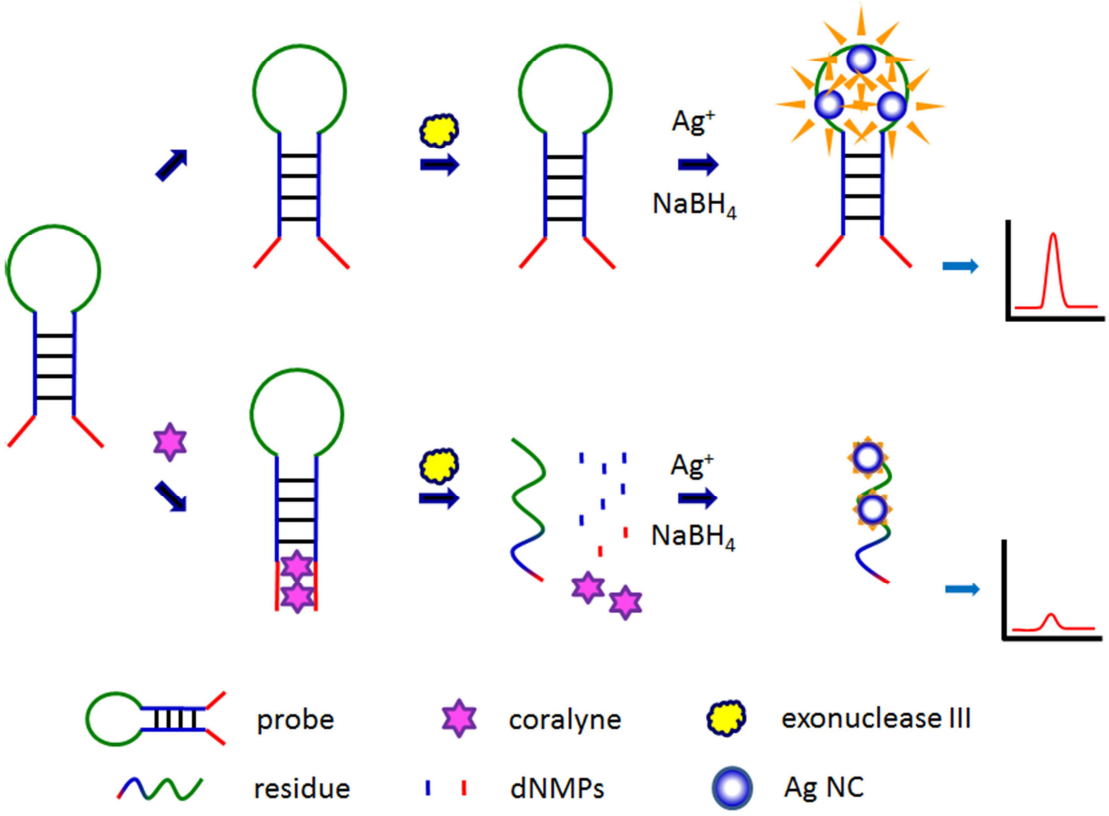

2

3 Scheme 1 Schematic representation of exonuclease III–based amplification in the
4 detection of coralyne.
5

2. Materials and methods

2.1 Chemicals and reagents

All chemicals were of reagent grade or higher. All stock and working solutions were prepared using Milli-Q deionized (DI) water (Millipore, Bedford, MA, USA) with a measured resistance of 18.2 MΩ·cm. Exonuclease III was purchased from US Biological Life Science (Salem, MA, USA). SYBR® green I was purchased from Invitrogen (St. Louis, MO, USA). Coralyne sulfoacetate, silver nitrate ($AgNO_3$), sodium tetrahydridoborate ($NaBH_4$), disodium hydrogen phosphate anhydrous, potassium dihydrogen phosphate, palmatine, and berberine were purchased from Sigma–Aldrich (St. Louis, MO, USA). Sanguinarine was purchased from Chengdu Biopurify Phytochemicals (Chengdu, China). The DNA probe having the sequence 5´-*AAA AAA* CGA TCC AAC GCC CCC CGC TTG GAT CG*A AAA AA*-3´ was purchased from MdBio (Taipei, Taiwan).

2.2 Apparatus

Fluorescence spectra were recorded using a Fluoromax-4 fluorescence spectrometer (Horiba, Kyoto, Japan). Field emission scanning electron microscopy (FE-SEM) was performed using a Jeol JSM-7401F instrument (Mitaka, Tokyo, Japan). Transmission electron microscopy (TEM) was performed using a JEM-2000FXII instrument (Mitaka, Tokyo, Japan). Particle size analysis was performed using Delsa Nano C apparatus (Billerica, MA, USA).

2.3 Detection of coralyne

The procedures for synthesizing oligonucleotide-stabilized Ag NCs were modified from those previously reported [37]. Probe DNA (100 μM, 5 μL) was placed in 1.5-mL Eppendorf tubes. Coralyne solutions (10 μL) of various concentrations were added and mixed with the probe DNA. Exonuclease III (20 U) was placed in the solutions, which

were then mixed, diluted with 1x reaction buffer to 100 μL, and left at 37 °C for 40 min. The mixture was heated to denature exonuclease III and, thereby, terminate the hydrolysis.

The Ag NCs were synthesized in the mixture solution through a procedure slightly modified from that reported previously [38]. After the mixture had cooled to room temperature, 1 mM $AgNO_3$ (8 μL) was added and the mixture was left for 30 min; 1 mM $NaBH_4$ (8 μL) was then added and the mixture was left for another 30 min to allow the synthesis of the oligonucleotide-stabilized Ag NCs. The resulting solution was placed in a fluorescence spectrometer for quantitation.

3. Results and discussion

3.1. Characterization of fabricated silver NCs

In the absence of coralyne, the DNA probe stabilized the Ag NCs, especially on the C-rich loop. Fig. 1(a) displays the SEM image of the Ag NCs. The particle size distribution of the Ag NCs [Fig. 1(b)] indicated that the average size of the Ag NCs was 1.5 ± 0.4 nm. Fig. 1(c) displays the corresponding excitation and emission spectra. In the presence of the C-rich loop, the synthesized Ag NCs exhibited a value of λ_{max} near 588 nm after excitation at a wavelength of 490 nm. These images and spectra confirmed the fabrication of the Ag NCs. Fig. S1 presents the particle sizes of the Ag NCs stabilized by ssDNA (primary average particle size: 37.4 ± 5.0 nm). The increase in particle size, compared with that of the particles stabilized by the DNA probe in the hairpin structure [as displayed in Fig. 1(b)], implies that the Ag NCs stabilized by the ssDNA residues had aggregated.

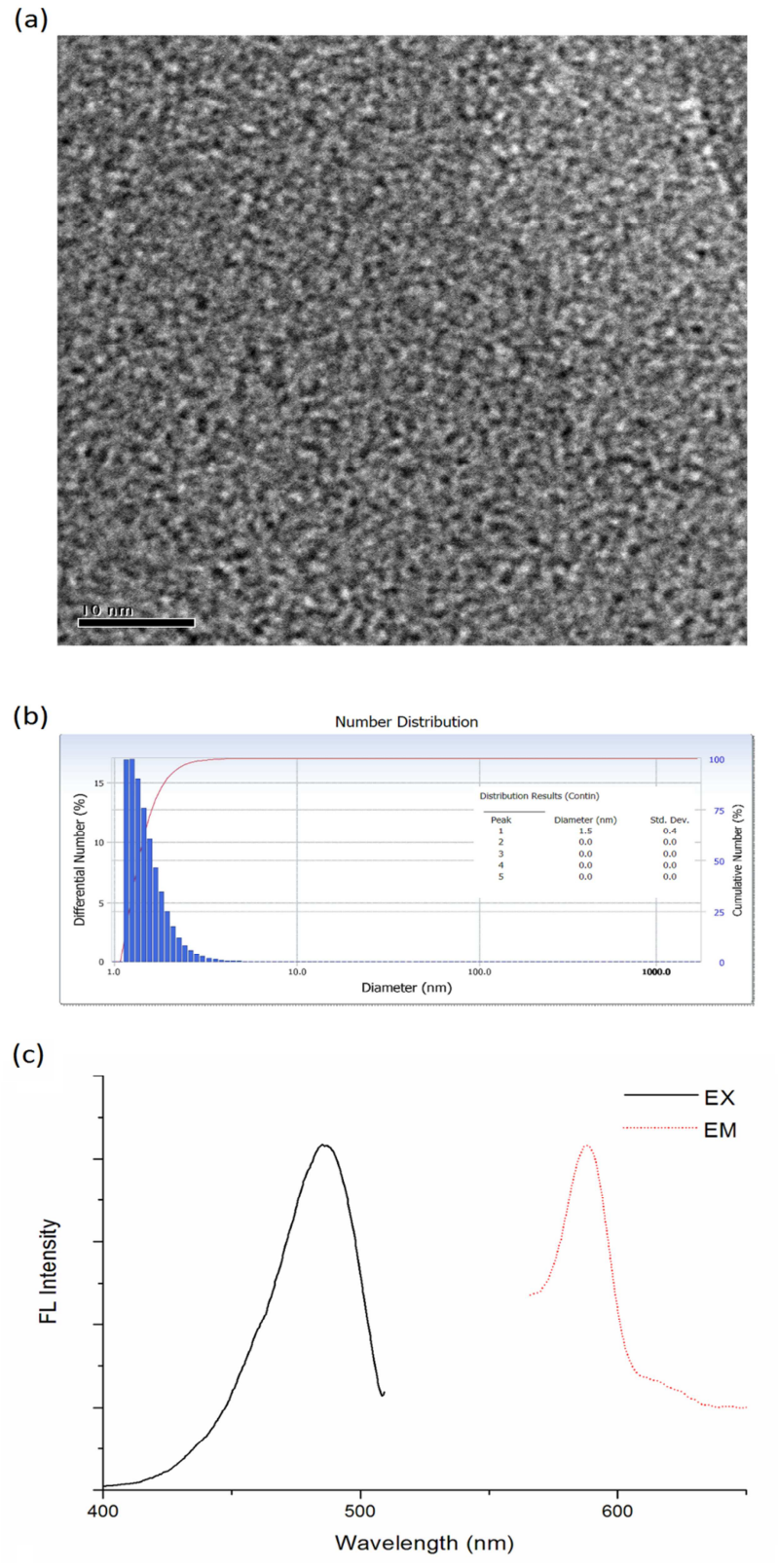

Fig. 1 (a) SEM image, (b) image from particle size analyzer, and (c) fluorescence spectra (black curve: excitation spectrum; red dotted curve: emission spectrum) of DNA-stabilized Ag NCs.

3.2. Detection of coralyne

Fig. 2 displays the fluorescence spectra of the Ag NCs on the DNA probe before (solid curve) and after (dotted curve) treatment with exonuclease III in the absence [Fig. 2(a)] and presence [Fig. 2(b)] of coralyne. When coralyne was absent, no changes in fluorescence intensity occurred before and after treatment with exonuclease III. We attribute this behavior to the poly-A section of the probe DNA maintaining a hairpin structure that could not be hydrolyzed by exonuclease III. Ag NCs were, therefore, synthesized in the C-rich sequence of the loop structure and their strong fluorescence emission was retained. When coralyne was present in the sample, the DNA probe bound with coralyne and closed the termini of the hairpin structure. Because the dsDNA structure remained prior to treatment with exonuclease III, the fluorescence spectra in the solid curve resembled the curves in Fig. 2(a). After exonuclease III had been added, the DNA probe was hydrolyzed, leaving the C-rich sequence to transform from a loop to an open ssDNA form. The fluorescence intensity of the Ag NCs synthesized from this ssDNA C-rich sequence was lower relative to that of the Ag NCs prepared from the DNA probe (hairpin structure), as reflected in the dotted curve in Fig. 2(b). The difference in fluorescence intensity between the two dotted lines in Fig. 2 could, therefore, be used to estimate the concentration of coralyne. Data from agarose gel electrophoresis [Fig. S2 (columns 1 to 4)] supported our claim that, in the presence of coralyne, non-Watson–Crick base-pairing between the poly-A termini of the DNA probe and coralyne resulted in hydrolysis of the DNA probe when subjected to exonuclease III digestion.

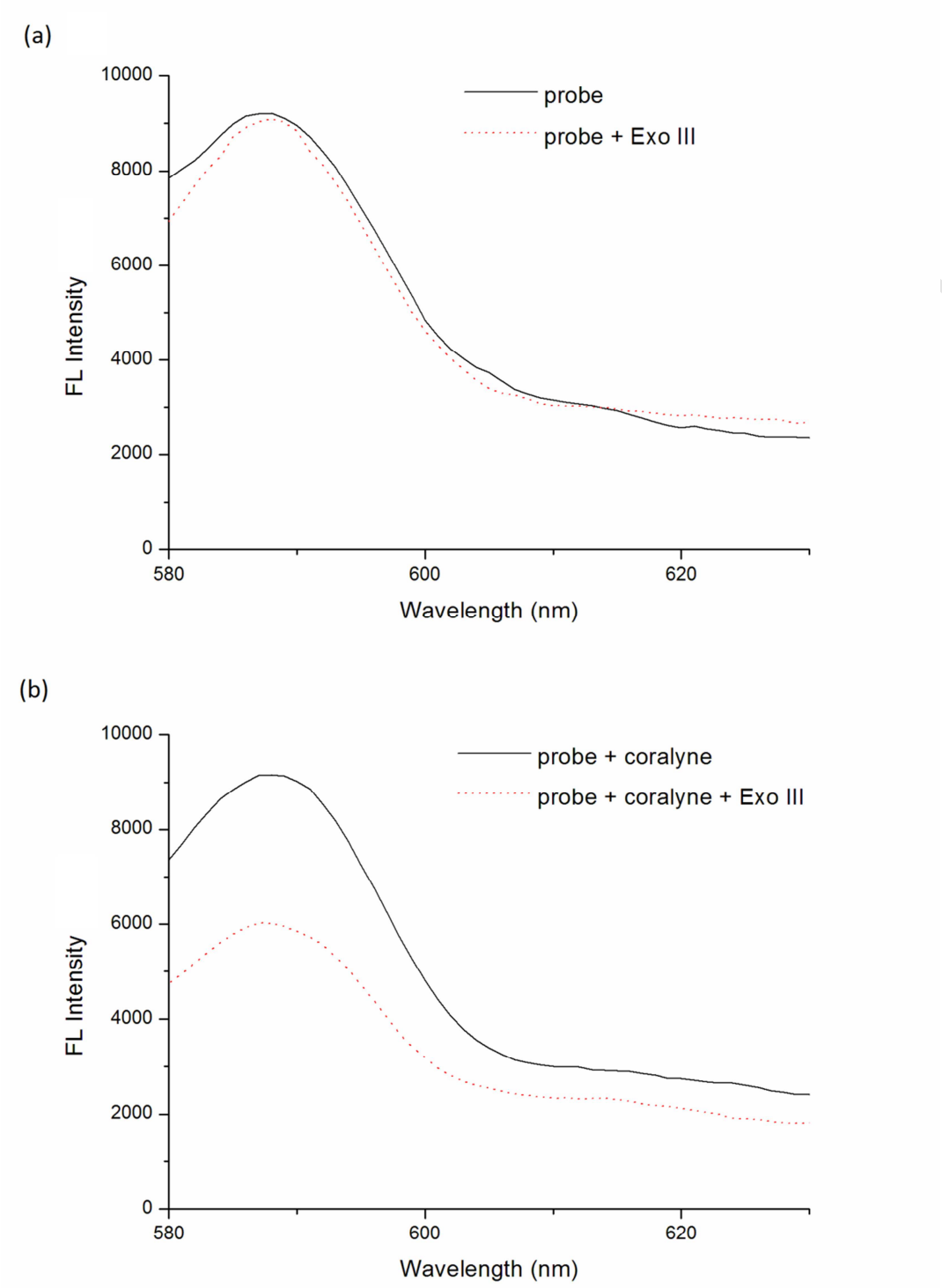

Fig. 2 Fluorescence spectra of Ag NCs before and after treatment with exonuclease III in the (a) absence and (b) presence of coralyne. Concentrations for the components: DNA probe, 5 μM; Exo III, 20 units; $AgNO_3$, 80 μM; $NaBH_4$, 80 μM.

3.3. Optimization of biosensor

We used the difference in fluorescence intensity of the oligonucleotide-stabilized Ag NCs to evaluate the concentration of coralyne. Because the fluorescence intensity was affected by the conditions of the Ag NC synthesis, these conditions were optimized to enhance the performance of the biosensor. Fig. 3(a) depicts the fluorescence intensity measured by the DNA probe (5 μM) in the presence of coralyne (100 nM) after various reaction times (5–120 min). At the beginning of the reaction, the fluorescence intensity decreased significantly, reflecting the rapid hydrolysis of the probe DNA bound with coralyne. The hydrolyzed DNA probe released the captured coralyne, triggering the binding/hydrolysis cycle of another molecule of the DNA probe. After 40 min, the fluorescence intensity became steady and low, indicating that most of the DNA probe had been hydrolyzed into the ssDNA form. Therefore, we chose a reaction time of 40 min for our subsequent experiments.

The morphology of oligonucleotide-stabilized Ag NCs can affect their optical properties. Therefore, we separately evaluated the effects of the concentrations of Ag^+ and $NaBH_4$ to determine how they influenced the particle sizes and/or distributions of the synthesized Ag NCs. The initial Ag^+ concentration was evaluated in the presence of a fixed amount of the DNA probe. Fig. 3(b) presents the fluorescence intensity plotted with respect to the Ag^+ concentration in the presence of the DNA probe (5 μM). The fluorescence intensity increased upon increasing the concentration of Ag^+ up to 80 μM. The increased fluorescence intensity presumably arose because more Ag NCs were synthesized upon increasing the concentration of Ag^+. Beyond 80 μM, the fluorescence intensity decreased, consistent with an excess of Ag^+ leading to larger Ag NCs that did not possess fluorescence properties. Therefore, an Ag^+ concentration of 80 μM was used in subsequent experiments.

Fig. 3(c) displays the effect of the $NaBH_4$ concentration. The fluorescence

intensity increased as we increased the $NaBH_4$ concentration from 20 to 80 μM, consistent with a higher $NaBH_4$ concentration favoring the synthesis of Ag NCs. The fluorescence intensity decreased, however, upon increasing the concentration of $NaBH_4$ beyond 80 μM, presumably because the free Ag^+ continued to undergo reduction on the fabricated Ag NCs, thereby enlarging the particle sizes and diminishing the fluorescence properties. Thus, a concentration of $NaBH_4$ of 80 μM was employed in the following experiments.

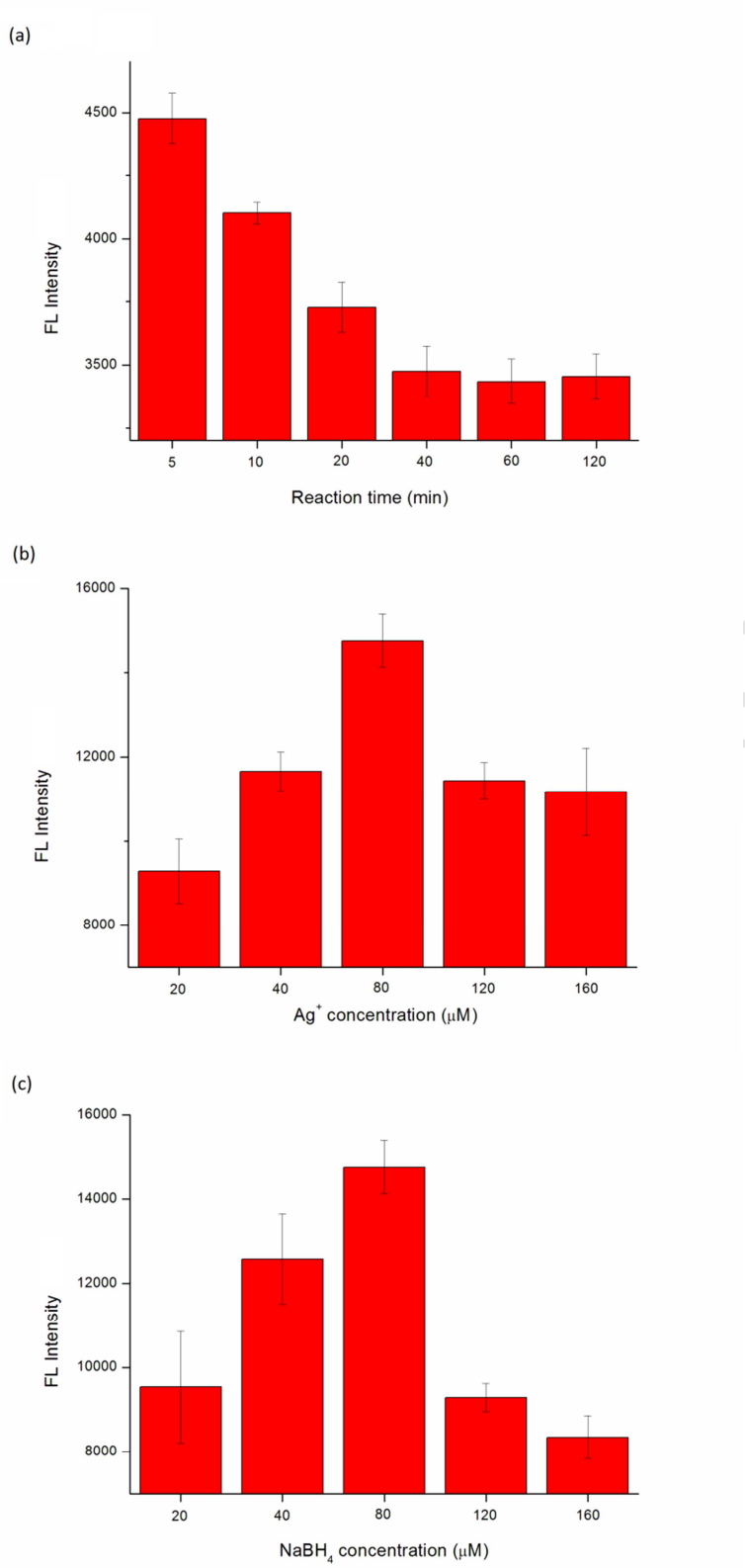

Fig. 3 Fluorescence intensities of Ag NCs measured after applying various (a) reaction times, (b) Ag^+ concentrations, and (c) $NaBH_4$ concentrations.

3.4. Sensitivity and selectivity of the coralyne biosensor

Fig. 4 displays the calibration curve of the coralyne biosensor, obtained under the optimized conditions. The relationship between the difference in fluorescence intensity (measured in the absence and presence of coralyne) and the concentration of coralyne (on a logarithmic scale) was linear within the range from 5 to 1000 nM, with a correlation of determination (R^2) of 0.99. The limit of detection (LOD) was 1.83 nM. Nevertheless, the inset to Fig. 4 (with the concentration of coralyne on a linear scale) reveals that the difference in the fluorescence intensity increased rapidly for low concentrations of coralyne, but increased slowly for high concentrations. Table S1 summarizes the analytical data for detecting coralyne, comparing those from previous studies with those from our present study.

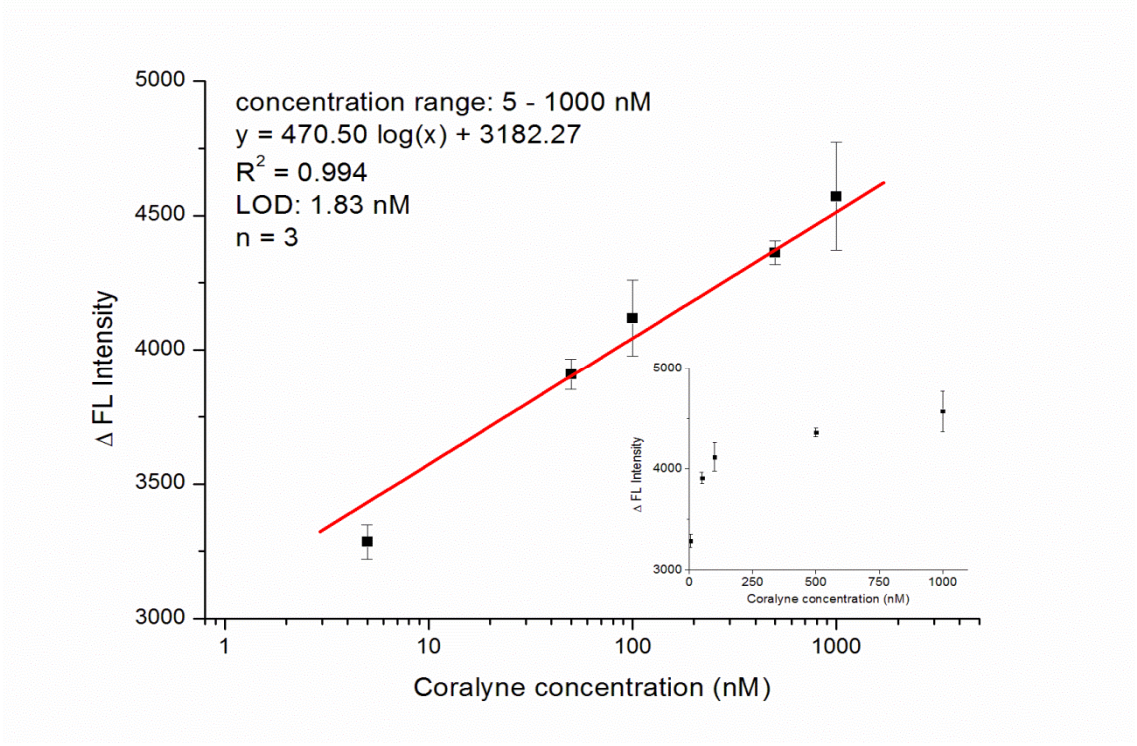

Fig. 4 Calibration curve (on a logarithmic scale) for the coralyne biosensor comprising the DNA probe (5 μM), $AgNO_3$ (80 μM), and $NaBH_4$ (80 μM). Inset: Change in fluorescence intensity for the detection of coralyne (on a linear scale) from 5 to 1000 nM.

To determine the selectivity of the coralyne biosensor, three other anti-cancer drugs (palmatine, berberine, sanguinarine), having structures similar to that of coralyne, were tested as interfering agents. Fig. 5 presents the changes in fluorescence intensity of the developed coralyne biosensor in the presence of these compounds. Relative to the change in fluorescence of the system containing 100 nM coralyne, the biosensor did not display any remarkable fluorescence responses even in the presence of 10-fold higher concentrations of these interfering agents. Moreover, a mixed sample solution containing 100 nM coralyne and 1 μM of each of the three interfering agents provided a response very similar to that of the solution containing only 100 nM coralyne, confirming the suitable selectivity of the coralyne biosensor. Because Hg^{2+} can undergo non-Watson–Crick base-pairing with thymine (T) [14], Hg^{2+} was employed here to further evaluate the selectivity of the DNA probe when using in this method. Fig. S2 (columns 5 and 6) presents the results obtained from agarose gel electrophoresis in the presence and absence of Hg^{2+} ions. The band in column 5, reflecting the DNA probe in the presence of Hg^{2+}, looks identical to the band of the DNA probe in column 1. The band in column 6 (DNA probe with Hg^{2+} in the presence of exonuclease III) has brightness similar to that in column 5, indicating that no digestion had occurred and that no interactions existed between Hg^{2+} and the free A bases in the DNA probe sequence. These findings provide further support for the high selectivity of our bioassay. We investigated the recoveries of this biosensor after spiking coralyne at 5 and 50 nM in untreated human urine. The recoveries were 88.01 and 101.31%, respectively, with relative standard deviations (RSDs) of less than 2.57%. Thus, the performance of our coralyne biosensor appears to be adequate for routine analysis.

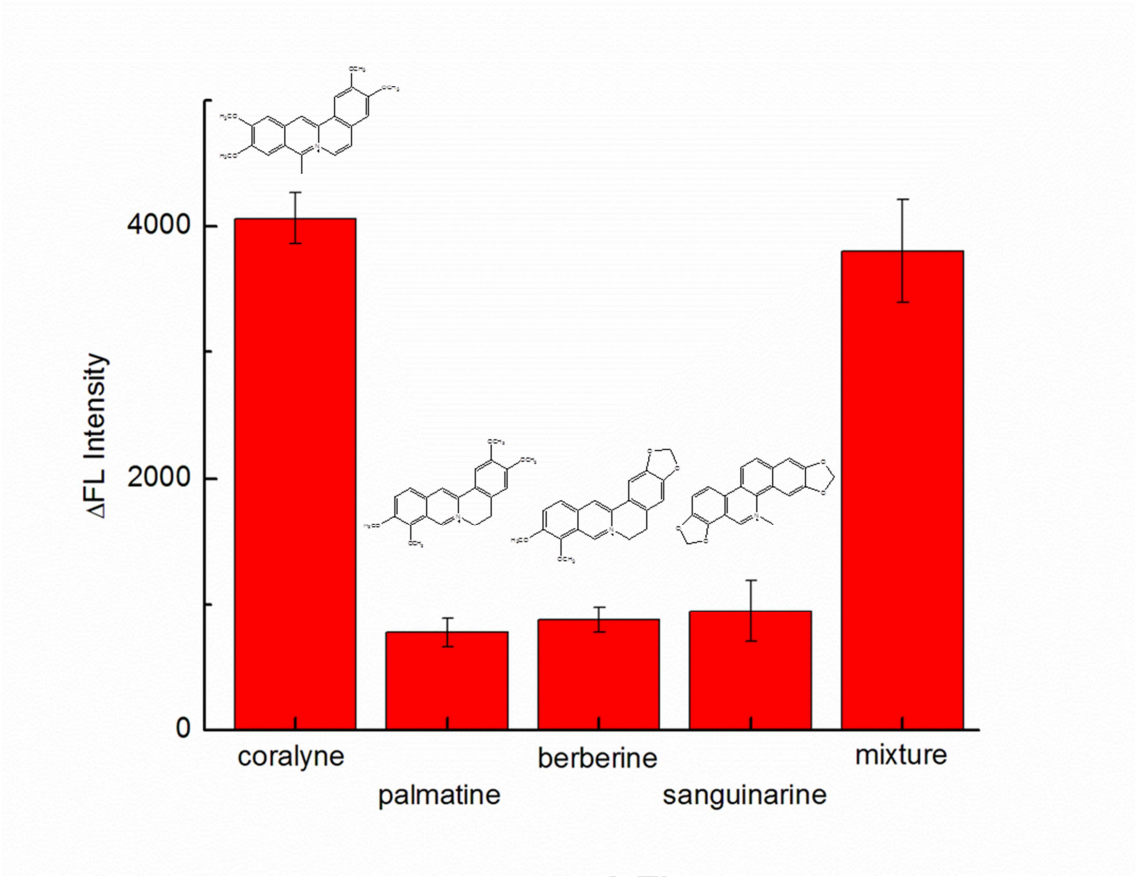

Fig. 5 Changes in fluorescence intensity of the coralyne biosensor in the presence of coralyne (100 nM), three other interfering agents (1 μM each), and a mixture of the four compounds.

4. Conclusions

We have constructed a biosensor for coralyne. In the presence of coralyne, the poly-A sequences at both ends of the probe hybridized in a specific manner with coralyne. Even though the coralyne molecule is far bigger than the ions (e.g., Hg^{2+}) reported to form non-Watson–Crick base pairing, and it would, therefore, lead to a larger distance between the two paired DNA sequences, the resulting A_2–coralyne–A_2 complex was still identified as a dsDNA by exonuclease III. After hydrolysis of the dsDNA mediated by exonuclease III, the liberated coralyne initiated the next step of cycling, resulting in the conformational changes—from hairpin to ssDNA

structures—of many probe species. Ag NCs displaying different fluorescence properties were synthesized in the presence and absence of coralyne. The difference in fluorescence intensity at 588 nm varied linearly with respect to concentration of coralyne (on a logarithmic scale) from 5 to 1000 nM. The estimated detection limit was 1.83 nM. This exonuclease III–based amplification strategy would appear to be applicable to other biosensor applications—on the condition that exonuclease III can recognize the non-Watson–Crick base pairing as a dsDNA.

Acknowledgments

This study was supported by a grant (MOST 105-2113-M-009-024) from the Ministry of Science and Technology and by the Center for Emergent Functional Matter Science of National Chiao Tung University from The Featured Areas Research Center Program within the framework of the Higher Education Sprout Project by the Ministry of Education (MOE) in Taiwan, R.O.C.

References

[1] J.-L. Gong, T. Sarkar, S. Badhulika, A. Mulchandani, Label-free chemiresistive biosensor for mercury (II) based on single-walled carbon nanotubes and structure-switching DNA, Appl. Phys. Lett., 102 (2013) 013701.

[2] N. Lu, C. Shao, Z. Deng, Colorimetric Hg^{2+} detection with a label-free and fully DNA-structured sensor assembly incorporating G-quadruplex halves, Analyst, 134 (2009) 1822-1825.

[3] G.-L. Wang, L.-Y. Jin, X.-M. Wu, Y.-M. Dong, Z.-J. Li, Label-free colorimetric sensor for mercury(II) and DNA on the basis of mercury(II) switched-on the oxidase-mimicking activity of silver nanoclusters, Anal. Chim. Acta, 871 (2015) 1-8.

[4] K. Jang, J. You, C. Park, S. Na, Highly sensitive detection of silver ions using a silver-specific DNA based nano-porous micro-resonator, New J. Chem., 41 (2017) 1840-1845.

[5] Y. Wu, R.Y. Lai, A reagentless DNA-based electrochemical silver(I) sensor for real time detection of Ag(I) - the effect of probe sequence and orientation on sensor response, Biotechnol. J., 11 (2016) 788-796.

[6] A. Dembska, The analytical and biomedical potential of cytosine-rich oligonucleotides: A review, Anal. Chim. Acta, 930 (2016) 1-12.

[7] P. Jain, B. Chakma, S. Patra, P. Goswami, Hairpin stabilized fluorescent silver nanoclusters for quantitative detection of NAD+ and monitoring NAD+/NADH based enzymatic reactions, Anal. Chim. Acta, 956 (2017) 48-56.

[8] C.-Y. Kuo, W.-L. Tseng, Adenosine-based molecular beacons as light-up probes for sensing heparin in plasma, Chem. Commun., 49 (2013) 4607-4609.

[9] K.S. Park, H.G. Park, A DNA-templated silver nanocluster probe for label-free, turn-on fluorescence-based screening of homo-adenine binding molecules, Biosens. Bioelectron., 64 (2015) 618-624.

[10] J.M. Wang, X.Y. Wang, S. Wu, J. Song, Y.Q. Zhao, Y.Q. Ge, C.G. Meng, Fabrication of highly catalytic silver nanoclusters/graphene oxide nanocomposite as nanotag for sensitive electrochemical immunoassay, Anal. Chim. Acta, 906 (2016) 80-88.

[11] A.Y. Khan, M. Hossain, G.S. Kumar, Investigations on the interaction of the phototoxic alkaloid coralyne with serum albumins, Chemosphere, 87 (2012) 775-781.

[12] T. Hou, X. Wang, X. Liu, S. Liu, Z. Du, F. Li, A label-free and colorimetric turn-on assay for coralyne based on coralyne-induced formation of peroxidase-mimicking split DNAzyme, Analyst, 138 (2013) 4728-4731.

[13] T. Hou, C. Li, X. Wang, C. Zhao, F. Li, Label-free colorimetric detection of coralyne utilizing peroxidase-like split G-quadruplex DNAzyme, Anal. Methods, 5

(2013) 4671-4674.
[14] H. Huang, S. Shi, X. Zheng, T. Yao, Sensitive detection for coralyne and mercury ions based on homo-A/T DNA by exonuclease signal amplification, Biosens. Bioelectron., 71 (2015) 439-444.
[15] B. Gatto, M.M. Sanders, C. Yu, H.Y. Wu, D. Makhey, E.J. LaVoie, L.F. Liu, Identification of topoisomerase I as the cytotoxic target of the protoberberine alkaloid coralyne, Cancer Res., 56 (1996) 2795-2800.
[16] F. Xing, G. Song, J. Ren, J.B. Chaires, X. Qu, Molecular recognition of nucleic acids: Coralyne binds strongly to poly(A), FEBS Lett., 579 (2005) 5035-5039.
[17] S.S. Jain, M. Polak, N.V. Hud, Controlling nucleic acid secondary structure by intercalation: effects of DNA strand length on coralyne-driven duplex disproportionation, Nucleic Acids Res., 31 (2003) 4608-4615.
[18] T.E. Du, Y.Y. Wang, Y. Zhang, T. Zhang, X. Mao, A novel adenosine-based molecular beacon probe for room temperature nucleic acid rapid detection in cotton thread device, Anal. Chim. Acta, 861 (2015) 69-73.
[19] G. Wang, Y. Zhu, L. Chen, X. Zhang, Dual hairpin-like molecular beacon based on coralyne-adenosine interaction for sensing melamine in dairy products, Talanta, 129 (2014) 398-403.
[20] J.S. Ren, J.B. Chaires, Sequence and structural selectivity of nucleic acid binding ligands, Biochemistry, 38 (1999) 16067-16075.
[21] Y.-H. Lin, W.-L. Tseng, Fluorescence detection of coralyne and polyadenylation reaction using an oligonucleotide-based fluorogenic probe, Chem. Commun., 47 (2011) 11134-11136.
[22] Y. Tao, Y.H. Lin, J.S. Ren, X.G. Qu, Self-assembled, functionalized graphene and DNA as a universal platform for colorimetric assays, Biomaterials, 34 (2013) 4810-4817.
[23] Y. Lu, Q. Huang, Label-free selective detection of coralyne due to aptamer-coralyne interaction using DNA modified SiO_2@Au core-shell nanoparticles as an effective SERS substrate, Anal. Methods, 5 (2013) 3927-3932.
[24] G. Song, C. Chen, X. Qu, D. Miyoshi, J. Ren, N. Sugimoto, Small-molecule-directed assembly: A gold nanoparticle-based strategy for screening of homo-adenine DNA duplex binders, Adv. Mater., 20 (2008) 706-710.
[25] J.T. Petty, J. Zheng, N.V. Hud, R.M. Dickson, DNA-templated Ag nanocluster formation, J. Am. Chem. Soc., 126 (2004) 5207-5212.
[26] V. Soto-Verdugo, H. Metiu, E. Gwinn, The properties of small Ag clusters bound to DNA bases, J. Chem. Phys., 132 (2010) 195102.
[27] E.G. Gwinn, P. O'Neill, A.J. Guerrero, D. Bouwmeester, D.K. Fygenson, Sequence-dependent fluorescence of DNA-hosted silver nanoclusters, Adv. Mater., 20 (2008) 279-283.

[28] M.L. Neidig, J. Sharma, H.C. Yeh, J.S. Martinez, S.D. Conradson, A.P. Shreve, Ag K-edge EXAFS analysis of DNA-templated fluorescent silver nanoclusters: insight into the structural origins of emission tuning by DNA sequence variations, J. Am. Chem. Soc., 133 (2011) 11837-11839.

[29] D. Schultz, K. Gardner, S.S.R. Oemrawsingh, N. Markesevic, K. Olsson, M. Debord, D. Bouwmeester, E. Gwinn, Evidence for rod-shaped DNA-stabilized silver nanocluster emitters, Adv. Mater., 25 (2013) 2797-2803.

[30] J.T. Petty, S.P. Story, S. Juarez, S.S. Votto, A.G. Herbst, N.N. Degtyareva, B. Sengupta, Optical sensing by transforming chromophoric silver clusters in DNA nanoreactors, Anal. Chem., 84 (2012) 356-364.

[31] T. Driehorst, P. O'Neill, P.M. Goodwin, S. Pennathur, D.K. Fygenson, Distinct conformations of DNA-stabilized fluorescent silver nanoclusters revealed by electrophoretic mobility and diffusivity measurements, Langmuir, 27 (2011) 8923-8933.

[32] P. Shah, S.W. Choi, H.J. Kim, S.K. Cho, Y.J. Bhang, M.Y. Ryu, P.W. Thulstrup, M.J. Bjerrum, S.W. Yang, Locking-to-unlocking system is an efficient strategy to design DNA/silver nanoclusters (AgNCs) probe for human miRNAs, Nucleic Acids Res., 44 (2016) e57.

[33] P.R. O'Neill, L.R. Velazquez, D.G. Dunn, E.G. Gwinn, D.K. Fygenson, Hairpins with poly-C loops stabilize four types of fluorescent Ag-n:DNA, J. Phys. Chem. C, 113 (2009) 4229-4233.

[34] C. Chen, Z. Yuan, H.-T. Chang, F. Lu, Z. Li, C. Lu, Silver nanoclusters as fluorescent nanosensors for selective and sensitive nitrite detection, Anal. Methods, 8 (2016) 2628-2633.

[35] F. Chen, J.J. Tu, C.S. Liang, B. Yang, C.Y. Chen, X.M. Chen, C.Q. Cai, Fluorescent drug screening based on aggregation of DNA-templated silver nanoclusters, and its application to iridium (III) derived anticancer drugs, Microchim. Acta, 183 (2016) 1571-1577.

[36] J.P. Zhang, C. Li, X. Zhi, G.A. Ramon, Y.L. Liu, C.L. Zhang, F. Pan, D.X. Cui, Hairpin DNA-Templated Silver Nanoclusters as Novel Beacons in Strand Displacement Amplification for MicroRNA Detection, Anal. Chem., 88 (2016) 1294-1302.

[37] L. Qi, Y. Huo, H. Wang, J. Zhang, F.Q. Dang, Z.Q. Zhang, Fluorescent DNA-protected silver nanoclusters for ligand-HIV RNA interaction assay, Anal. Chem., 87 (2015) 11078-11083.

[38] Q. Cao, Y. Teng, X. Yang, J. Wang, E. Wang, A label-free fluorescent molecular beacon based on DNA-Ag nanoclusters for the construction of versatile Biosensors, Biosens. Bioelectron., 74 (2015) 318-321.

(a)

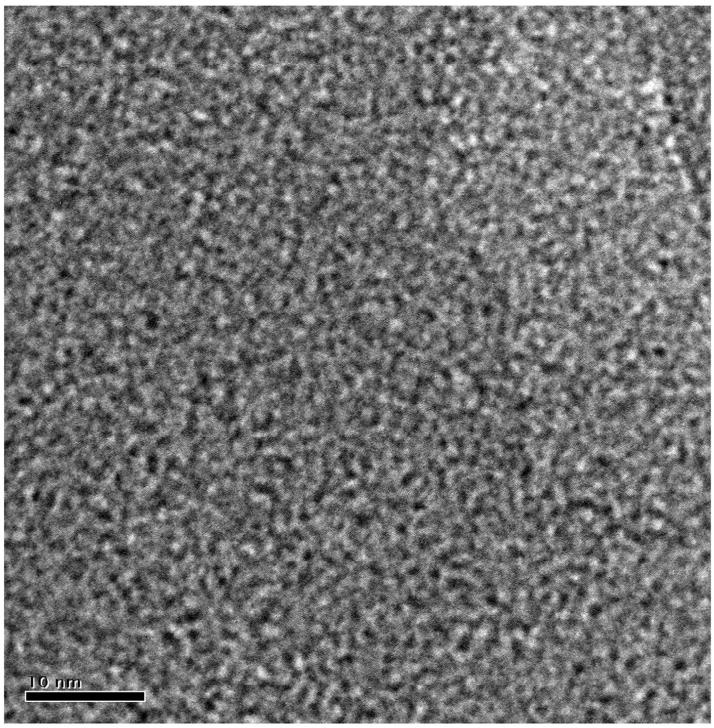
10 nm

(b)

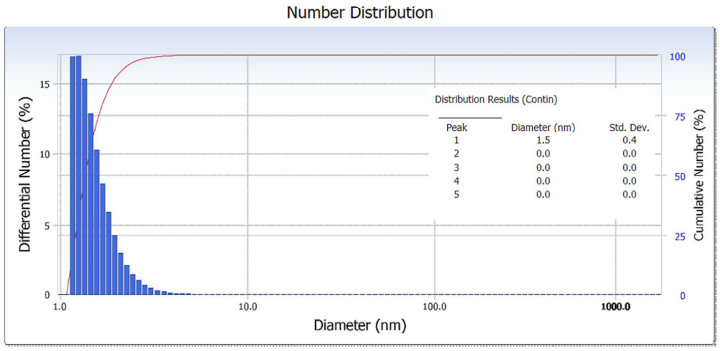
Number Distribution
Differential Number (%)
Cumulative Number (%)
Diameter (nm)
Distribution Results (Contin)
Peak Diameter (nm) Std. Dev.
1 1.5 0.4
2 0.0 0.0
3 0.0 0.0
4 0.0 0.0
5 0.0 0.0

(c)

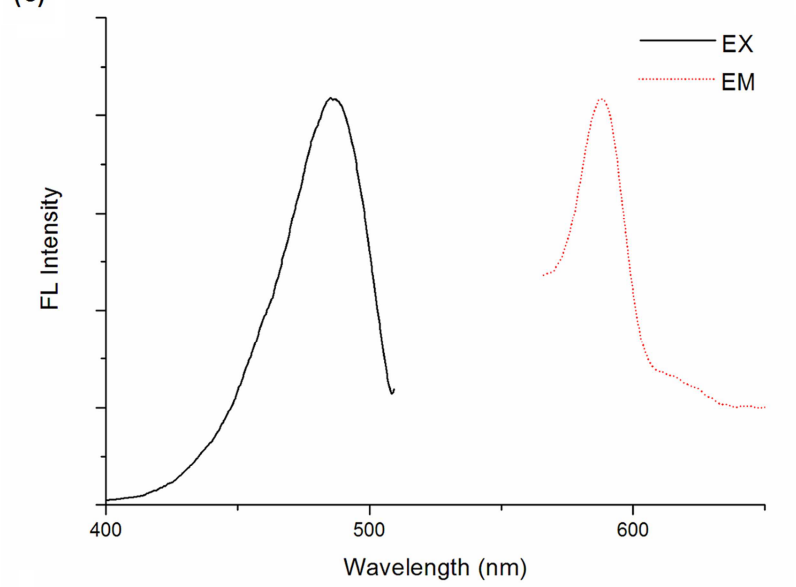
EX
EM
FL Intensity
Wavelength (nm)

(a)

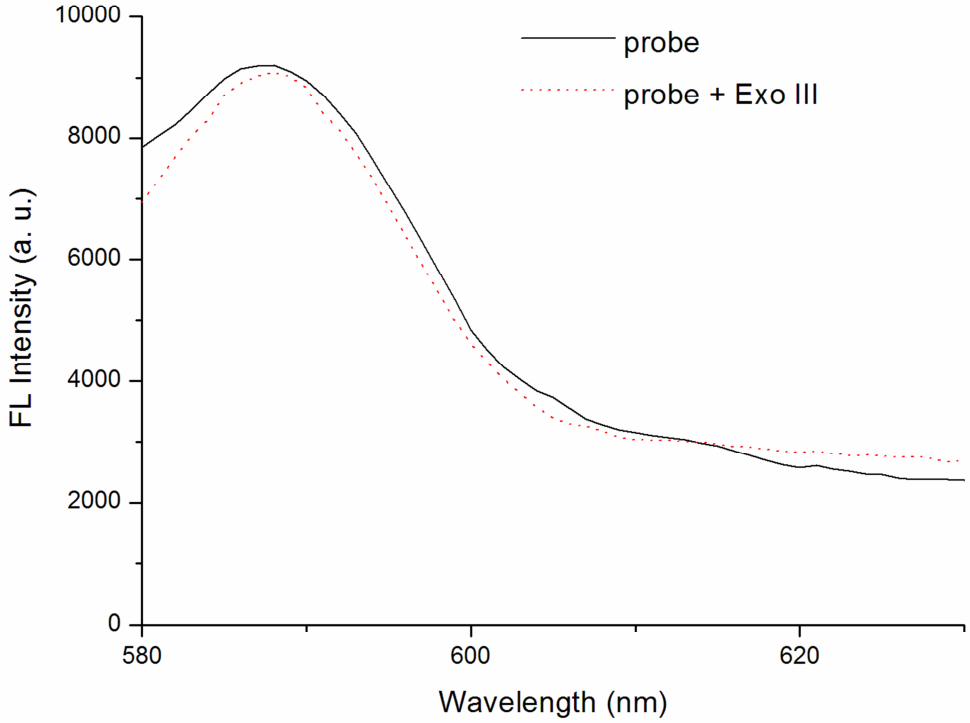
probe
probe + Exo III
FL Intensity (a. u.)
Wavelength (nm)
0
2000
4000
6000
8000
10000
580
600
620

(b)

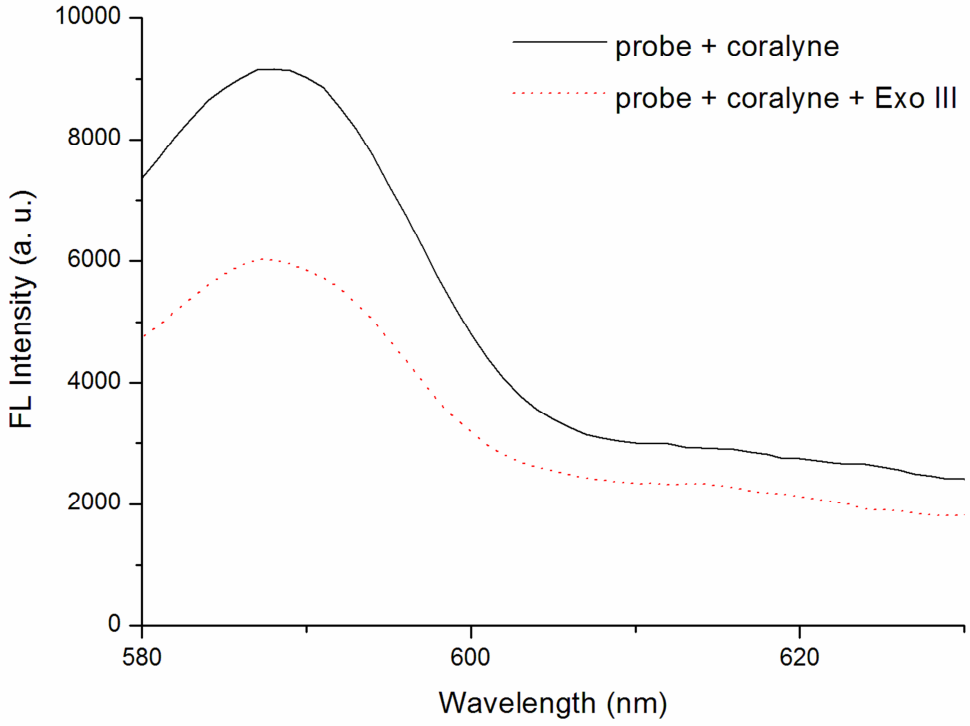
probe + coralyne
probe + coralyne + Exo III
FL Intensity (a. u.)
Wavelength (nm)
0
2000
4000
6000
8000
10000
580
600
620

(a)

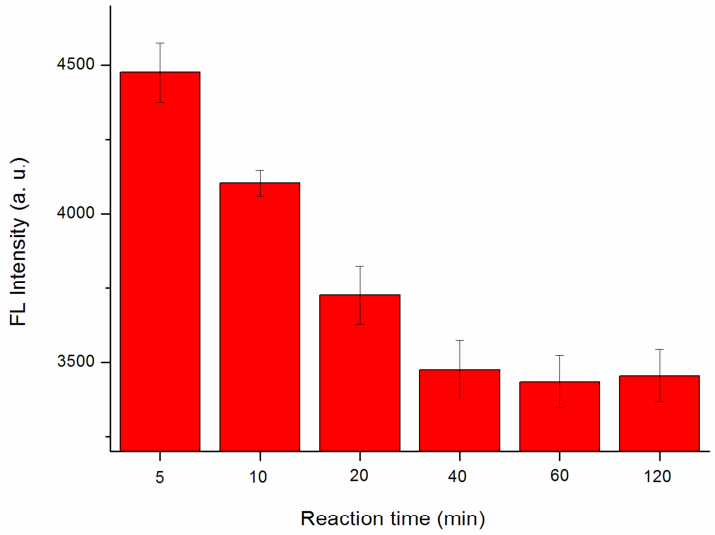
FL Intensity (a. u.)
4500
4000
3500
5
10
20
40
60
120
Reaction time (min)

(b)

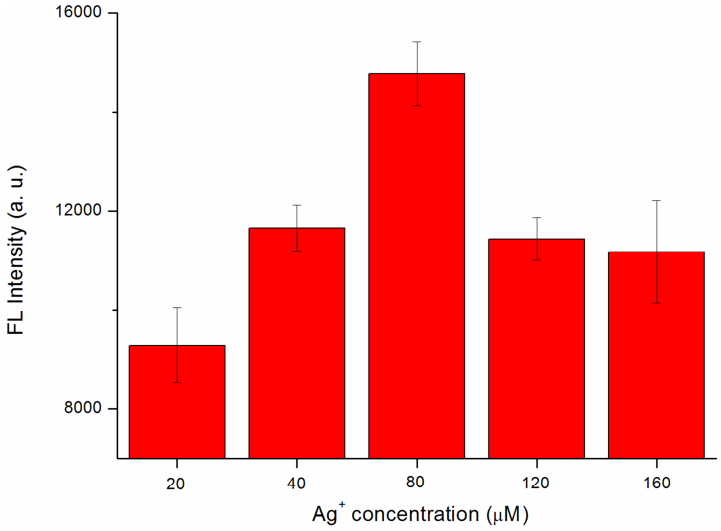
FL Intensity (a. u.)
16000
12000
8000
20
40
80
120
160
Ag+ concentration (μM)

(c)

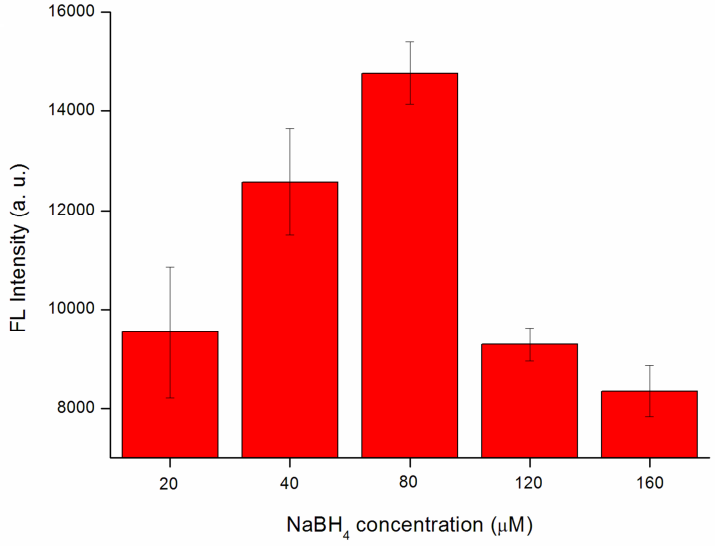
FL Intensity (a. u.)
16000
14000
12000
10000
8000
20
40
80
120
160
NaBH4 concentration (μM)

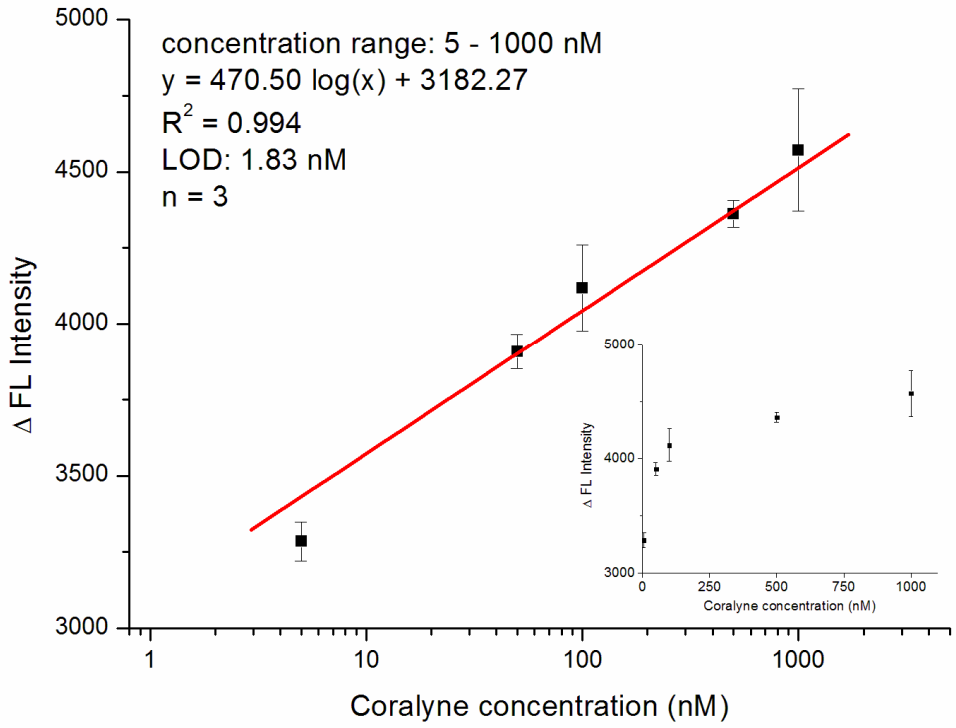

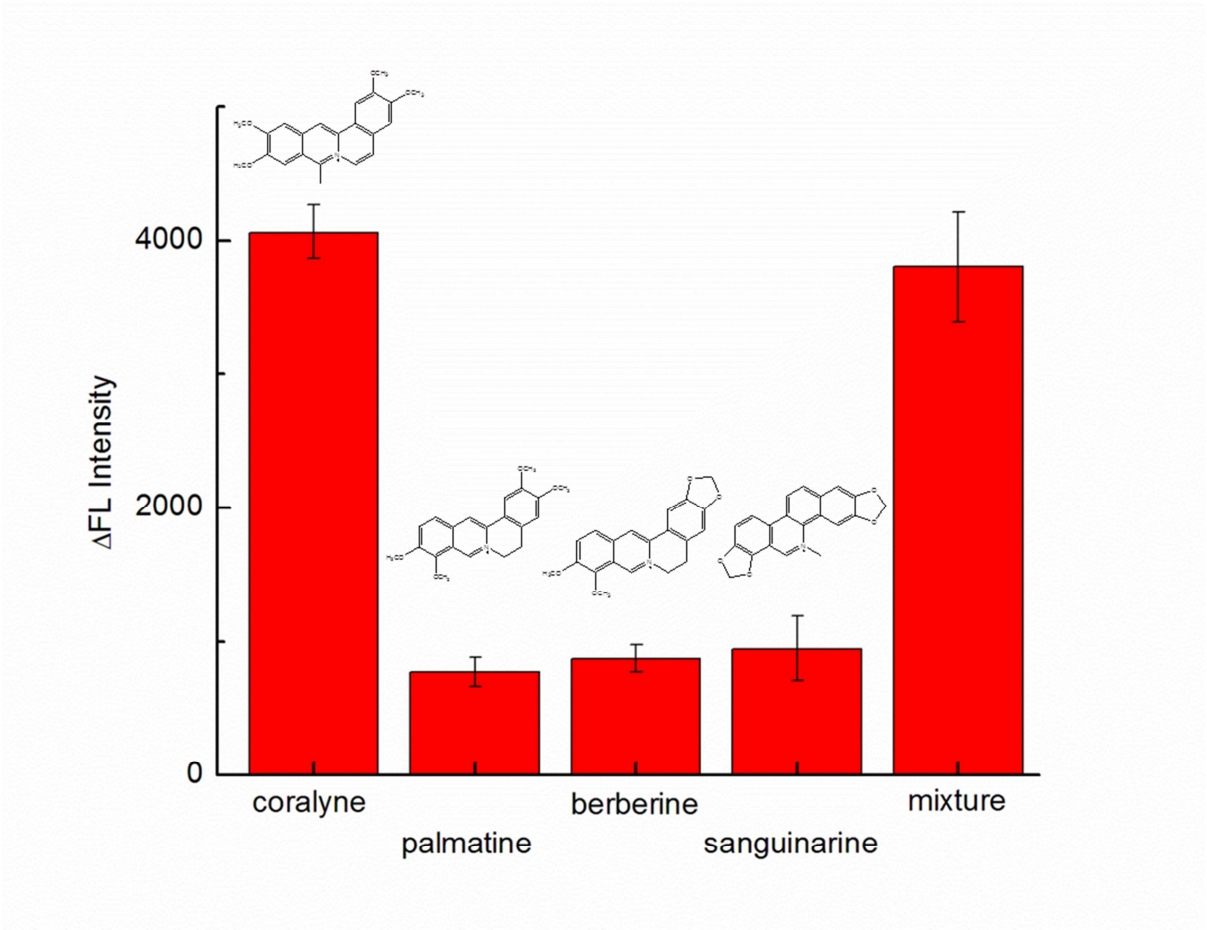

Highlights

1. A label-free biosensor has been developed to detect coralyne.

2. Silver nanoclusters (Ag NCs) were synthesized with the help of the DNA probe.

3. Fluorescence sensitivity was enhanced using exonuclease III amplification.

4. The LOD was 1.83 nM of the biosensor appears suitable for the analysis of coralyne.